

## Origin of mechanoluminescence from Mn-activated ZnAl<sub>2</sub>O<sub>4</sub>: Trielectricty-induced electroluminescence

Hiroaki Matsui,\* Chao-Nan Xu,† Yun Liu, and Hiroshi Tateyama

*National Institute of Advanced Industrial Science and Technology, AIST, Kyushu, Tosu, Saga 841-0052, Japan*

(Received 21 January 2004; published 24 June 2004)

Luminescence induced by friction, mechanoluminescence (ML) has been observed for ZnAl<sub>2</sub>O<sub>4</sub>: Mn<sup>2+</sup> (ZAO:Mn) fabricated by systematically controlling the reducing temperature. The reducing treatment produced lattice defects under a reducing atmosphere. Those defects were associated with Zn and O vacancies through evaporation of ZnO in ZnAl<sub>2</sub>O<sub>4</sub>, which was trapped with a large amount of carrier in the spinel. Results of dependence of ML intensity and integrated intensity for thermoluminescence on the reducing temperature showed that the trapped carrier plays an important role in producing the ML for ZAO:Mn. In addition, the ML for ZAO:Mn was strongly dependent upon the friction rod material; it was closely related to the surface voltage generated in the vicinity of the frictional surface. These results suggest that the ML for ZAO:Mn was caused by the effect of triboelectrification, but not piezoelectricity because ZnAl<sub>2</sub>O<sub>4</sub> has a centrosymmetric structure (*Fd3m*). Therefore, the carrier that is trapped in the spinel can be excited by the local electric field derived from friction between the two dissimilar materials, where the excited carrier is accelerated toward the luminescent center of the Mn<sup>2+</sup> ions. Consequently, the Mn<sup>2+</sup> ions are excited and release an emission band on the transition from <sup>4</sup>T<sub>1</sub> to <sup>6</sup>A<sub>1</sub>. Evidence for these physical processes was corroborated from the finding that reduced ZAO:Mn showed highly efficient electroluminescence (EL). Therefore, it is inferred that the ML for ZAO:Mn is caused by triboelectricity-induced EL.

DOI: 10.1103/PhysRevB.69.235109

PACS number(s): 78.60.Kn, 78.60.Mq, 61.72.Ji, 71.55.Ht

### I. INTRODUCTION

Mechanoluminescence (ML) is an interesting phenomenon whereby mechanical energies such as compression, friction, and fracture are converted directly to “light.” Heretofore, investigations concerning ML have been carried out using various kinds of materials such as inorganic and organic solids, and metals.<sup>1–10</sup> These investigations show that ML is closely involved in the physical processes that can typically be divided into two types: (1) deformation-ML and (2) tribo-ML. The former results from physical processes induced during deformation of solids, whereas the latter results from contact phenomena such as triboelectrification and tribochemical reactions induced during contact between two dissimilar materials. Deformation ML depends only on the material subjected to deformation and not on the material used to produce the deformation and the contact phenomenon. In contrast, tribo-ML is dependent on the nature of the materials under deformation in addition to the type of materials used to produce the deformation; it arises solely because of contact phenomena.

We previously investigated the use of ML materials such as novel self-diagnosis systems, optical stress sensors, and stress image devices.<sup>11–13</sup> Therefore, it is desirable to further our understanding of complicated ML processes in an effort to find new ML materials from oxide material systems possessing endurance against severe environments. We recently documented intensive ML induced during friction of ZnAl<sub>2</sub>O<sub>4</sub>: Mn<sup>2+</sup> (ZAO:Mn) annealed at 1300°C in a reducing atmosphere. Thereby, large amounts of carrier for trapping centers were formed in the ZnAl<sub>2</sub>O<sub>4</sub>.<sup>14</sup> Use of other spinel oxides has shown that MgGa<sub>2</sub>O<sub>4</sub>:Mn<sup>2+</sup> and ZnGa<sub>2</sub>O<sub>4</sub>:Mn<sup>2+</sup> displayed higher ML intensities than

MgAl<sub>2</sub>O<sub>4</sub>:Mn<sup>2+</sup> and that the ML intensity was associated closely with the content of the trapped carrier in the spinels.<sup>15</sup> Our previous studies indicated that the trapped carrier plays an important role in producing intensive ML from spinel oxides. This role also holds for other ML oxide such as SrAl<sub>2</sub>O<sub>4</sub>:Eu<sup>2+</sup>.<sup>12,16</sup>

The friction-induced ML for ZAO:Mn was similar to that of ZnS:Mn<sup>2+</sup>, although ZAO:Mn showed no ML under deformation. It has been reported that ZnS:Mn, which is classified as a deformation ML, displays highly efficient ML originating from piezoelectricity and electroluminescence (EL).<sup>17</sup> However, given that the ZnAl<sub>2</sub>O<sub>4</sub> possesses a crystal structure with cubic symmetry (*Fd3m*), it possesses no piezoelectricity. Our previously published work confirmed that the ML for ZAO:Mn was caused by the 3*d* transition between <sup>4</sup>T<sub>1</sub> and <sup>6</sup>A<sub>1</sub> of Mn<sup>2+</sup> ions because PL and ML spectra showed emission peaks at 512 nm.<sup>14</sup> Unfortunately, it remains unclear which physical processes are indispensable for transference from the friction energy to Mn<sup>2+</sup> ions as the luminescence center, a process that is important as a driving force for producing the intensive ML from ZAO:Mn. Therefore, we investigated ML for ZAO:Mn systematically by controlling the reducing temperature in an effort to clarify the origin of the ML. As a result, we found that fabrication of intensive ML for ZAO:Mn was indispensable in yielding a large amount of trapped carrier, triboelectricity, and highly efficient EL, which are all important aspects for understanding the physical processes of ML for ZAO:Mn.

In this study, we initially investigate the characteristics of ZAO:Mn annealed at various temperatures in a reducing atmosphere. These investigations are achieved through analysis of crystal structure, photoluminescence (PL), thermoluminescence (ThL), and ML as a first step in clarifying the

origin of ML. We then comment on physical processes of the ML for ZAO:Mn, including other spinel oxides. The present study adds to our understanding of the ML of ZAO:Mn and will assist in future applications of ML produced from spinel oxides.

## II. EXPERIMENT

$\text{Zn}_{0.995}\text{Al}_2\text{O}_4:\text{Mn}_{0.005}$  (ZAO:Mn) samples were synthesized by a solid-state reaction consisting of two firing stages because ZnO, when used as a starting material, sublimes violently in a reducing atmosphere.<sup>18</sup> High-purity ZnO (99.99%),  $\text{Al}_2\text{O}_3$  (99.999%), and  $\text{MnCO}_3$  (99.9%) powders in a composition ratio of  $(\text{Zn}_{0.995}, \text{Mn}_{0.005})\text{Al}_2\text{O}_4$  were mixed thoroughly in ethanol, dried at 90°C for 12 h, and then subjected to grinding. The resultant powders were fired at 1250°C for 8 h in air. Single phase ZAO:Mn was then reduced at various temperature for 4 h in the range of 900–1300°C under 5%  $\text{H}_2$  diluted in Ar ambient to reduce manganese ions from  $\text{Mn}^{3+}$  to  $\text{Mn}^{2+}$ . The color of the powder samples changed from brown to white when the manganese ions were reduced to  $\text{Mn}^{2+}$ . Results of photoluminescence excitation spectroscopy<sup>14,15</sup> showed that manganese ions are located in the tetra coordination of the  $\text{Zn}^{2+}$  site in the spinel structure.

Crystal structures were examined by x-ray diffraction (XRD) measurements using Cu  $K\alpha$  line (RINT 2000; Rigaku Corp.). Investigations of structural stability during the reduction process were measured using thermo-gravimetry (TG) with a heating rate of 10°C/min. Two types of samples were used in this study. One sample was made employing molding, where 3.5 g of optical epoxy resin was mixed with 1 g of powder sample to form a  $\phi 25 \times 15$  mm pellet. The other sample consisted of sintered pellets possessing a size of  $\phi 20 \times 1$  mm. The sintered pellets were fabricated by cold isostatic pressing at 2000 kg/cm<sup>2</sup> followed by heat treatment in a reducing atmosphere. Friction was applied using a friction rod under a load on the rotating sample. Details of this technique have been reported previously.<sup>19</sup> The ML intensity was measured using a computer system that incorporated a photo-multiplier tube (R464; Hamamatsu Photonics, K.K.) and a photon counter (C5410; Hamamatsu Photonics, K.K.). The measured emission wavelength range of this system was 300–650 nm. The ML spectrum was measured using a photon multichannel analyzer (PMA 100; Hamamatsu Photonics, K.K.). The spectra of PL and EL at room temperature (RT) were investigated using a fluorescence spectrometer (FP-6500, Jasco Inc.) equipped with an optical fiber attachment and double monochromators. The evaluation of glow curves for ThL was the same as that used in measuring the PL and EL spectra and recorded from RT to 300°C at a heating rate of 0.18°C/s.

## III. RESULTS AND DISCUSSION

### A. Structural analysis, photoluminescence, and thermoluminescence

Figure 1 shows XRD patterns of ZAO:Mn after reduction at various temperatures. The samples reduced at 900, 1000,

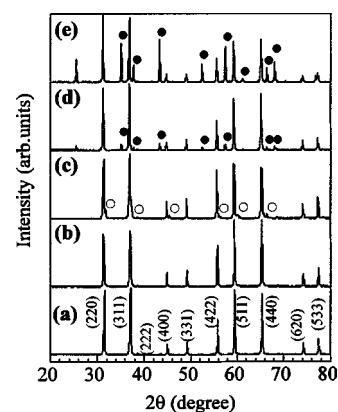


FIG. 1. XRD patterns of ZAO:Mn after reduction at various temperatures. XRD patterns (a), (b), (c), (d), and (e) represent results for nonreduction and reduction at 900–1100, 1200, 1250, and 1300°C, respectively. Symbols of ○ and ● show the defective spinel structure of Zn-Al-O and the corundum structure of  $\alpha\text{-Al}_2\text{O}_3$ , respectively.

and 1100°C had a single phase structure of  $\text{ZnAl}_2\text{O}_4$ , whereas the samples reduced above 1200°C possessed two types of an impurity phase in addition to the spinel phase. The impurity phase in the sample reduced at 1200°C can be related to the presence of a Zn-poor defective spinel structure with Zn-Al-O composition because the XRD peaks shifted slightly to the higher angles from the main peaks of the spinel. Yan *et al.* observed a similar result for  $\text{ZnGa}_2\text{O}_4$  annealed in a reducing atmosphere.<sup>20</sup> Furthermore, it is known that the lattice constant in the spinel structure ( $\text{AB}_2\text{O}_4$ ) decreased with increasing deficiency of cations in A sites; consequently, the diffraction peaks of the spinel phase shifted to the higher angles.<sup>18,21</sup> On the other hand, the samples reduced at 1250–1300°C had an  $\alpha\text{-Al}_2\text{O}_3$  phase typical of a corundum structure. These results indicate that ZnO in  $\text{ZnAl}_2\text{O}_4$  evaporated from the spinel structure during heating in the reducing atmosphere; as a result, the  $\alpha\text{-Al}_2\text{O}_3$  remained by way of a metastable structure of Zn-Al-O structure. This evaporation process was confirmed from the weight loss of  $\text{ZnAl}_2\text{O}_4$  observed by TG measurement, as shown in Fig. 2. The weight loss began in the neighborhood of 900°C. Large losses were observed at temperatures above

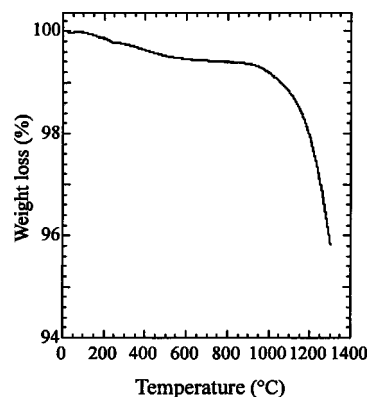


FIG. 2. TG curve of ZAO:Mn during heating in a reducing atmosphere at a rate of 10°C/min.

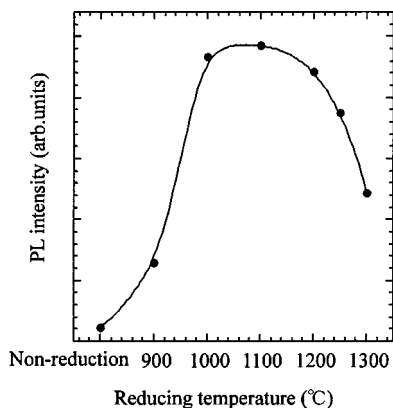


FIG. 3. Dependence of PL intensity on reducing temperature for ZAO:Mn. PL was measured under an excitation wavelength of 457 nm.

1200°C. We estimated the lattice constant from the peaks related to the spinel phase for the samples reduced at 900–1300°C using a standard Si substance. The lattice constant of all the reduced samples was  $8.084 \pm 0.001$  Å, suggesting that all the reduced samples possessed the same  $\text{ZnAl}_2\text{O}_4$  spinel structure.

The PL of ZAO:Mn displayed an emission peak at 512 nm under excitation wavelength of 457 nm originating from  ${}^4T_1$  to  ${}^6A_1$  transition of the  $\text{Mn}^{2+}$  ions located in the tetra coordination  $\text{Zn}^{2+}$  site of the spinel structure.<sup>22,23</sup> Figure 3 displays temperature dependence of PL intensity on the reducing temperature for ZAO:Mn. The PL intensity increased with increasing reducing temperature up to 1100°C. It then decreased above 1200°C. The presence of maximum PL intensity for the sample reduced at 1100°C is attributable to the suitable reducing conditions of manganese ions from  $\text{Mn}^{3+}$  to  $\text{Mn}^{2+}$ . On the other hand, the decrease in PL intensity for the samples reduced above 1200°C is attributable to the partial destruction of the spinel structure, as indicated by XRD and TG results.

The reduced  $\text{ZnAl}_2\text{O}_4$  is expected to produce lattice defects of zinc and oxygen vacancies as a result of long-lasting phosphorescence with an emission peak at 512 nm. It is known that lattice defects can act as trapping centers of carrier (holes or electrons). It is also known that the amount of carrier trapped in lattice defects can be evaluated qualitatively from the integrated intensity of the glow curve obtained by ThL measurement. Figure 4(a) shows glow curves of ZAO:Mn reduced at 900, 1000, and 1200°C. All samples were annealed initially up to 300°C to release carrier trapped in the lattice defects. They were irradiated with ultraviolet (UV) light of 365 nm for 5 min at RT before ThL measurement. The ThL measurement was started after 2 h to prevent thermal fading at RT. Samples reduced at 900°C showed a glow curve with a peak at 110°C, whereas glow curves for samples reduced at 1000 and 1200°C possessed a wide emission peak around 150 and 220°C. The glow curves are closely associated with the type of trapping levels of carrier formed in the  $\text{ZnAl}_2\text{O}_4$ . The difference of the glow curves between the samples reduced at 900 and above 1000°C indicated that different trapping levels had formed in the host after the reducing process. Herein, the glow curves for ZAO:Mn can be explained as follows.

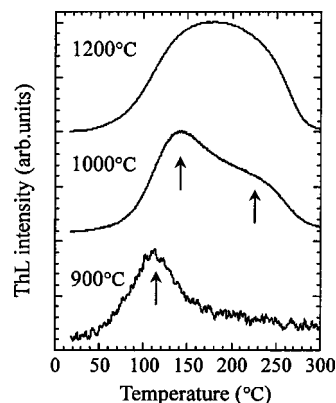


FIG. 4. Glow curves for ZAO:Mn reduced at 900, 1000, and 1200°C, respectively. The heating rate was 0.18°C/s.

Manganese ions are partially oxidized from  $\text{Mn}^{2+}$  to  $\text{Mn}^{3+}$  when sintered as ZAO:Mn in air. Ziolkowski *et al.* suggested that occupation sites and valence fluctuation of  $\text{Mn}^{2+}$  and  $\text{Mn}^{3+}$  in  $\text{Zn}_{1-x}\text{Mn}_x\text{Al}_2\text{O}_4$  engendered production of lattice defects in the spinel.<sup>24</sup>



where  $\phi$  indicates lattice defects. Furthermore, Inoue *et al.* have suggested that the valence of manganese ions introduced to the spinel block was 2.472 in  $\text{Ba}_{0.75}\text{Al}_{10.706}\text{Mn}_{0.254}\text{O}_{17.25}$  with  $\beta$ -alumina structure fabricated in air.<sup>25</sup> From the result of PL shown in Fig. 3, the reduction from  $\text{Mn}^{3+}$  to  $\text{Mn}^{2+}$  ions is insufficient in the ZAO:Mn sample reduced at 900°C, which was confirmed from the presence of an absorption peak attributed to the transition of  $\text{Mn}^{3+}$  ions by UV-VIS spectrometer. The incorporation of rare earth (Re) ions into ZnO and ZnS engenders lattice defects, such as oxygen and sulfur vacancies resulting from the uncharged valence between  $\text{Zn}^{2+}$  and  $\text{Re}^{3+}$  ions.<sup>26,27</sup> If the glow peak for ZAO:Mn reduced at 900°C was caused by lattice defects attributable to a complex of  $\text{Mn}^{3+}$  and vacancy, then it can be understood that the disappearance of the glow peak at 110°C for the ZAO:Mn reduced at 1000 and 1200°C resulted from the full reduction of  $\text{Mn}^{3+}$  to  $\text{Mn}^{2+}$  ions. On the other hand, the wide glow peak at around 150–250°C must have been produced from lattice defects related to the host atoms, such as zinc and oxygen vacancies generated through evaporation of ZnO from  $\text{ZnAl}_2\text{O}_4$  in the reducing atmosphere.

Figure 5 shows the dependence of ThL integrated intensity on reducing temperature for ZAO:Mn. The ThL integrated intensity increased with increasing reducing temperature up to 1250°C; it then decreased at 1300°C. Apparently, the ThL integrated intensity increased steeply from 1100°C, which can be related to XRD and TG results. That is, the partial destruction of the spinel structure following annealing at reducing temperatures above 1200°C resulted in the formation of lattice defects related to the host atoms, which were able to trap large amounts of carrier by UV irradiation. Koumoto *et al.* reported that Zn vacancies are produced in

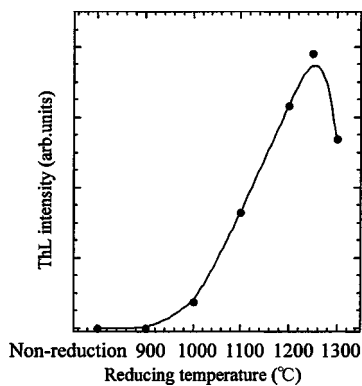


FIG. 5. Dependence of ThL integrated intensity on reducing temperature for ZAO:Mn.

ZnAl<sub>2</sub>O<sub>4</sub> through sublimation of ZnO from the host from the studies detailing evaporation processes of ZnO from ZnAl<sub>2</sub>O<sub>4</sub> in a reducing atmosphere using a Knudsen molecular flood technique.<sup>28</sup> This behavior can be understood qualitatively from XRD, TG, and ThL measurements in this work.

In this section, we determined that the reduced ZAO:Mn possessed a large amount of trapped carrier resulting from evaporation of ZnO from ZnAl<sub>2</sub>O<sub>4</sub> caused by the reducing process. The trapping levels of carrier were associated closely with lattice defects of the host atoms such as zinc and oxygen vacancies. Further investigations using x-ray photoemission and electron-spin-resonance spectroscopy are required to ascertain the type of lattice defects.

**B. Mechanoluminescence and its luminescence mechanism**

Figure 6 shows the ML intensity of ZAO:Mn reduced at various temperatures in the range of 900–1300°C. The loading force was 2.1 N and the rotation velocity of the sample was 2.8 cm/s. Samples were irradiated with an UV light at 365 nm for 5 min prior to ML measurement; moreover, they were kept in a darkened room for 2 days to achieve thermal equivalence. The dependency of ML intensity on reducing temperature for ZAO:Mn was similar to that of the depen-

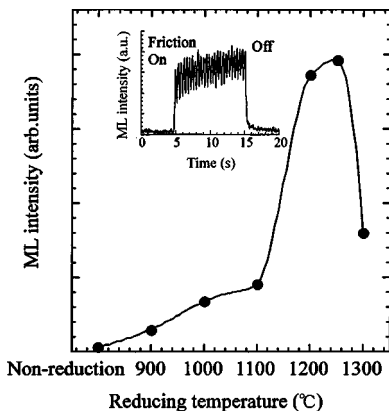


FIG. 6. Dependence of ML intensity on reducing temperature for ZAO:Mn. ML was measured after an interval of 2 days following UV excitation. The inset displays a typical ML response signal measured at 2.1 N and 2.8 cm/s.

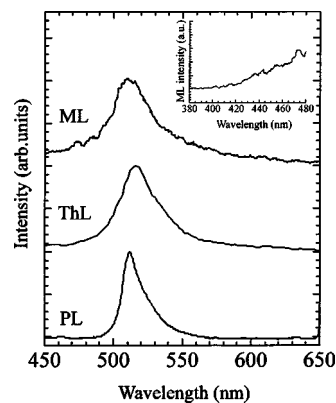


FIG. 7. Emission spectra of PL, ThL, and ML for ZAO:Mn. The inset shows the emission spectrum in the narrow regions from 380 to 480 nm for the ML.

dependency of integrated intensity for ThL, as shown in Fig. 5. The maximum ML intensity was obtained after reduction at temperatures of 1200 and 1250°C. Figure 6 (inset) shows that the ML response curve remained flat without marked decreases in intensity during measurement, which was similar to ZnS:Mn<sup>2+</sup> but different from SrAl<sub>2</sub>O<sub>4</sub>:Eu<sup>2+</sup>.<sup>29</sup> Oscillation in ML intensity during friction correlated with the rotation velocity of 8.6 cm/s. It may have occurred because of the nonuniformity of the samples. The ML intensity was reproducible. In addition, it increased linearly with increasing friction force. We investigated the ML properties of  $\alpha$ -Al<sub>2</sub>O<sub>3</sub>:Mn because an  $\alpha$ -Al<sub>2</sub>O<sub>3</sub> phase was observed in the XRD patterns of the ZAO:Mn reduced above 1250°C. As a result,  $\alpha$ -Al<sub>2</sub>O<sub>3</sub>:Mn showed no clear light emission by friction. Therefore, the high ML intensity for ZAO:Mn can be attributed to the amount of carrier trapped by the lattice defects produced in the spinel structure, as suggested from the dependency of the reduction temperature on ML intensity and integrated intensity for ThL.

Figure 7 shows the PL, ThL, and ML for ZAO:Mn. Each spectrum showed an emission peak around 512 nm, indicating that the ML for ZAO:Mn was produced by the optical transition of Mn<sup>2+</sup> ions. It has been reported that triboemission results from gas discharges of the ambient atmosphere, especially N<sub>2</sub>, which is present in the vicinity of the frictional surface.<sup>30,31</sup> This implies that Mn<sup>2+</sup> ions may be excited by photons with emission peaks at 399, 406, and 427 nm arising from the nitrogen gas discharge. However, emission peaks of the nitrogen gas discharge were not observed from the ML spectrum, as shown in the inset of Fig. 7. Longchambon *et al.*, in studies concerning the fracture of quartz, demonstrated the presence of ML spectra with a wide emission peak from 430 to 480 nm with nitrogen gas discharge lines.<sup>32</sup>

The ML of ZAO:Mn is affected by phosphorescence resulting from UV irradiation. Trapping levels that consist of shallow and deep traps cause phosphorescence. Figure 8(a) shows the dependence of ML intensity on reducing temperature for ZAO:Mn measured after a 3-min interval following UV irradiation. The ML intensity measured after the 3 min interval was two orders of magnitude higher than that measured after an interval of 2 days, as shown in Fig. 8(a). The

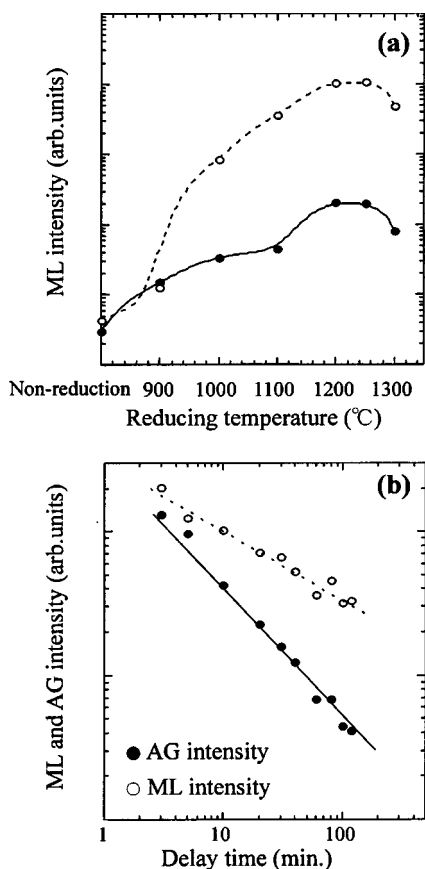


FIG. 8. (a) Dependence of ML intensity on reducing temperature for ZAO:Mn. The ML was measured after an interval of 3 min (○) and 2 days (●) following UV excitation. (b) Decay curves of ML and AG intensities for the ZAO:Mn reduced at 1200°C as a function of delay time following UV irradiation.

ML intensity decreased with decreasing afterglow (AG) intensity, as shown in Fig. 8(b). However, the emission intensity recovered following further UV irradiation. That indicates that the ML for ZAO:Mn induced by friction stimulated carrier trapped in the shallow levels was related to the phosphorescence. That is, the ML of ZAO:Mn was not caused by fractoluminescence occurring by the local surface fracture following nitrogen gas discharges, which can also be concluded from the result that the ML intensity was dependent on the integrated intensity for ThL.

It has been said that friction between dissimilar materials produces charge electrification in the vicinity of the frictional surface,<sup>33</sup> which is comprehensively called triboelectromagnetism and can be classified as tribo-ML. For instance, the luminescence produced during low-energy impact of steel or a sapphire needle on alkali halide crystals is tribo-ML because the intensity is dependent on the material of the rod used for impact and on the contact potential between the two materials.<sup>34</sup> Furthermore, the ML produced during separation of a tape from a substrate is dependent on both the nature of the tape and the substrate. It occurs by triboelectrification.<sup>35,36</sup> The ML property for ZAO:Mn is dependent on the material of the friction rod. Figure 9(a) shows the ML intensity of ZAO:Mn ceramics produced by various types of friction rods. The polycarbonate, polyethylene, and

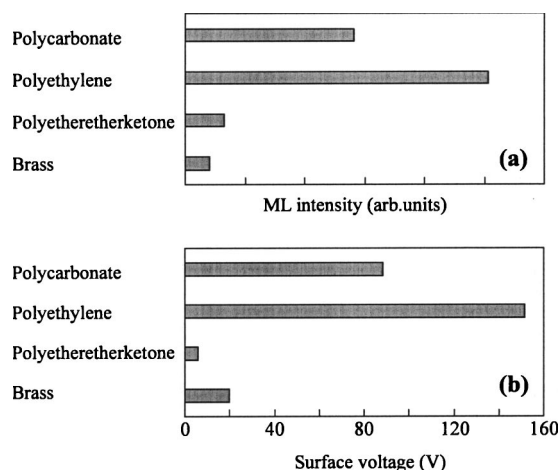


FIG. 9. The ML intensity (a) and surface voltage (b) plotted against several kinds of friction rods.

polyetheretherketone (PEEK) plastics and brass metal were chosen as friction rod materials. The contact area between each friction rod and the sample was kept in the range of 6.0–6.6 mm<sup>2</sup>. Results of the ML shown in Figs. 6 and 8 were measured using a polyethylene rod. Figure 9(a) indicates that the polycarbonate and polyethylene friction rods had higher ML intensities than the PEEK and metal rods. Furthermore, we confirmed that surface voltage was generated during the ML measurement from measurements of a noncontact surface voltmeter, as shown in Fig. 9(b), and that the ML intensity was dependent on surface voltage generated during the friction. These results imply that the origin of ML for ZAO:Mn is associated with triboelectrification resulting from the friction of two dissimilar materials.

ZnGa<sub>2</sub>O<sub>4</sub>: Mn<sup>2+</sup> and MgGa<sub>2</sub>O<sub>4</sub>: Mn<sup>2+</sup> are known to show highly efficient EL.<sup>37–39</sup> When a strong electric field is applied to the sample, carrier is excited from deep traps formed in a lattice through Pool-Frenkel and tunnel emission processes and becomes hot carrier by applying a strong electric field. Consequently, luminescent center ions are excited by hot electrons and thereby emit. It is generally believed that EL properties for phosphor materials activated by luminescent centers such as transition and rare earth ions are the result of these processes. The EL properties for ZAO:Mn were investigated by applying an alternating current (60 Hz, 1.5 kV) to transparent (ITO) and Al electrodes on both faces of the ZAO:Mn ceramic ( $\phi 20 \times 1$  mm). Figure 10 shows the EL spectrum and response signal for the ZAO:Mn ceramic reduced at 1200°C. The EL spectrum showed an emission peak at 512 nm that was based on the optical intratransition between the 3d orbital of the Mn<sup>2+</sup> ions. On the other hand, the EL was not observed for the ZAO:Mn that was reduced at 900°C.

The ML for ZnS:Mn has been accounted for in terms of a piezoelectrification induced EL model because noncentrosymmetric ZnS possesses piezoelectricity and shows highly efficient EL. However, the ML for ZAO:Mn could not be attributed to piezoelectrification. Recently, Ronfard-Haret *et al.* reported that the grinding-induced ML for rare-earth-ion-doped ZnO ceramics was involved in the characteristic EL observed.<sup>40,41</sup> Taking the EL results into account,

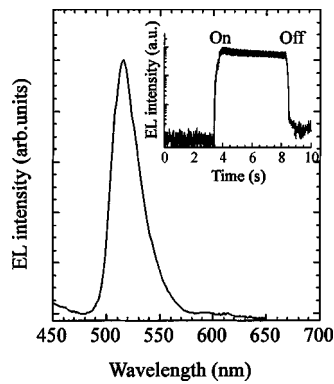


FIG. 10. EL spectrum measured by applying an alternating voltage. The inset shows a typical EL response curve.

the ML for centrosymmetric ZAO:Mn can be accounted for in terms of a triboelectricity-induced EL model. Figure 11 shows a schematic model depicting the mechanism of the ML in ZAO:Mn. When friction is applied on ZAO:Mn, the carrier trapped in the spinel can be excited by the local electric field originating from triboelectrification arising from the friction between two dissimilar materials because the EL observed for ZAO:Mn is associated with the carrier trapped in the host. Thereafter, the excited carrier is converted to hot carrier with high energy that is accelerated toward the luminescent center of  $\text{Mn}^{2+}$  ions. Subsequently, the  $\text{Mn}^{2+}$  ions were excited and thereby released an emission band on the transition from  ${}^4T_1$  to  ${}^6A_1$ .

Finally, we should note that the ML for  $\text{MgGa}_2\text{O}_4:\text{Mn}^{2+}$  (MGO:Mn) and  $\text{ZnGa}_2\text{O}_4:\text{Mn}^{2+}$  (ZGO:Mn) can be accounted for in terms of the triboelectricity-induced EL model. MGO:Mn and ZGO:Mn can form a large number of trapping centers of carrier using the reducing technique and can show highly efficient EL. Consequently, we also confirmed that the ML for MGO:Mn and ZGO:Mn were dependent on friction rod materials in the same way as the ML for ZAO:Mn.

#### IV. CONCLUSIONS

Intensive ML was observed during application of a friction on the spinel ZAO:Mn annealed in a reducing atmosphere at temperatures of 1200–1250°C. Reducing temperatures above 1200°C engendered a higher content of lattice defects related to zinc and oxygen vacancies through evapo-

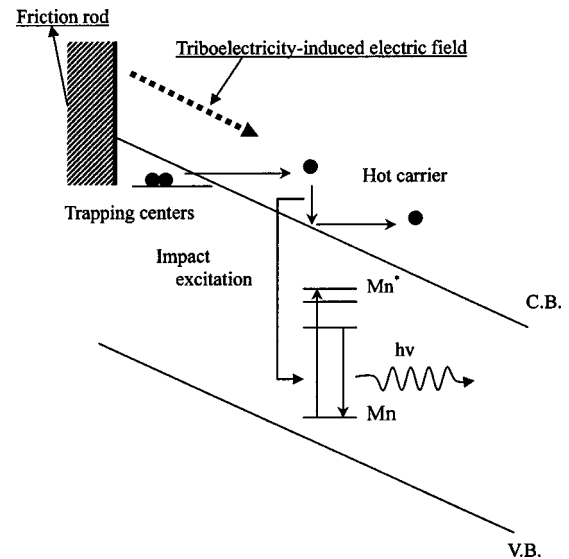


FIG. 11. A schematic model depicting the mechanism of ML in ZAO:Mn.

ration of ZnO in  $\text{ZnAl}_2\text{O}_4$  under a reducing atmosphere. That situation could create trapping centers for large amounts of carrier into the spinel. The ML intensity increased with increasing carrier trap content. That observation was confirmed through analysis of ThL and phosphorescence originating from shallow and deep traps. Taking into account the dependency of ML intensity on the friction rod material, the ML for ZAO:Mn can be considered to have been produced not by fractoluminescence, but by the effect of triboelectrification. The absence of emission peaks associated with nitrogen gas discharges and the generation of surface voltage near the frictional surface support that inference. Further, the reduced ZAO:Mn showed highly efficient EL. Therefore, it is suggested that the ML for centrosymmetric ZAO:Mn without piezoelectricity, which differs from that of noncentrosymmetric ZnS:Mn, can be accounted for in terms of the triboelectricity-induced EL model. In ZAO:Mn, friction as mechanical energy and light was connected through the complete physical processes of triboelectricity and EL; the ML intensity can be controlled by the content of the trapping centers of carrier formed in the spinel. Results of this study are expected to contribute importantly toward future investigations concerning the ML in spinel materials and other oxide material systems.

\*Present address: The Institute of Scientific and Industrial Research, Osaka University, Mihogaoka 8-1, Ibaraki, Osaka 567-0047, Japan.

†Author to whom correspondence should be addressed. PRESTO, Japan Science and Technology Corporation (JST), Honcho, Kawaguchi, Saitama 332-0012, Japan. Electronic address cnxu@aist.go.jp

<sup>1</sup>N. A. Atari, Phys. Lett. **90A**, 93 (1992).

<sup>2</sup>G. N. Chapman and A. J. Walton, J. Phys. C **16**, 5543 (1983).

<sup>3</sup>Y. Chem, M. M. Abraham, J. J. Turner, and C. M. Nelson, Philos. Mag. **32**, 99 (1975).

<sup>4</sup>G. P. Williams, Jr. and J. J. Turner, Solid State Commun. **29**, 201 (1979).

<sup>5</sup>R. Alzetta, I. Chudacek, and R. Scarmozzino, Phys. Status Solidi A **1**, 775 (1970).

<sup>6</sup>T. Ishihara, K. Tanaka, K. Fujita, K. Hirao, and N. Soga, Solid

- State Commun. **107**, 763 (1998).
- <sup>7</sup>B. P. Chandra, *Radiat. Eff. Defects Solids* **138**, 119 (1996).
- <sup>8</sup>L. M. Sweeting, M. L. Cashel, and M. M. Rosenblatt, *J. Lumin.* **52**, 281 (1992); *J. Phys. Chem.* **92**, 5688 (1988).
- <sup>9</sup>G. T. Reynolds, *J. Lumin.* **75**, 295 (1997).
- <sup>10</sup>J. T. Dickinson, E. E. Donaldson, and M. K. Park, *J. Mater. Res.* **16**, 2897 (1981).
- <sup>11</sup>C. N. Xu, T. Watanabe, M. Akiyama, P. Sun, and X. G. Zheng, *J. Am. Ceram. Soc.* **82**, 2342 (1999).
- <sup>12</sup>C. N. Xu, T. Watanabe, M. Akiyama, and X. G. Zheng, *Appl. Phys. Lett.* **74**, 1236 (1999).
- <sup>13</sup>C. N. Xu, X. G. Zheng, M. Akiyama, K. Nonaka, and T. Watanabe, *Appl. Phys. Lett.* **76**, 179 (2000).
- <sup>14</sup>H. Matsui, C. N. Xu, and H. Tateyama, *Appl. Phys. Lett.* **78**, 1068 (2001).
- <sup>15</sup>H. Matsui, C. N. Xu, M. Akiyama, and T. Watanabe, *Jpn. J. Appl. Phys., Suppl.* **39**, 6582 (2000).
- <sup>16</sup>C. N. Xu, in *Encyclopedia of Smart Materials*, edited by M. Schwartz (Wiley, New York, 2002), Vol. 1, p. 190.
- <sup>17</sup>C. N. Xu, H. Matsui, Y. Liu, X. G. Zheng, and L. Y. Li, *Ferroelectrics* **263**, 3 (2001).
- <sup>18</sup>K. Shirasuka, G. Yamaguchi, and Y. Miyachi, *Yogyo Kyokaishi* **84**, 14 (1976).
- <sup>19</sup>C. N. Xu, X. G. Zheng, T. Watanabe, M. Akiyama, and I. Usui, *Thin Solid Films* **352**, 273 (1999).
- <sup>20</sup>Z. Yan, H. Takei, and H. Kawazoe, *J. Am. Ceram. Soc.* **81**, 180 (1998).
- <sup>21</sup>E. Proverbio, M. Yasuoka, K. Hirao, and S. Kanzaki, *J. Ceram. Soc. Jpn.* **101**, 256 (1993).
- <sup>22</sup>S. D. Mo and W. Y. Ching, *Phys. Rev. B* **54**, 16555 (1996).
- <sup>23</sup>D. T. Palumbo and J. J. Brown, Jr., *J. Electrochem. Soc.* **117**, 1184 (1970).
- <sup>24</sup>J. Ziolkowski, A. M. Maltha, H. Kist, E. J. Grootendorst, H. J.M. de Groot, and V. Ponec, *J. Catal.* **160**, 148 (1996).
- <sup>25</sup>H. Inoue, M. Machida, K. Eguchi, and H. Arai, *J. Mater. Chem.* **6**, 455 (1996).
- <sup>26</sup>Y. Qian, K. Hara, H. Munekata, and H. Kukimoto, *Jpn. J. Appl. Phys., Part 2* **34**, L368 (1995).
- <sup>27</sup>Y. Hayashi, H. Narahara, T. Uchida, T. Noguchi, and S. Ibuki, *Jpn. J. Appl. Phys., Part 1* **34**, 1878 (1995).
- <sup>28</sup>K. Kumoto, S. Mizuta, and H. Yanagita, *Yogyo Kyokaishi* **88**, 217 (1980).
- <sup>29</sup>C. N. Xu, T. Watanabe, M. Akiyama, and X. G. Zheng, *Appl. Phys. Lett.* **74**, 2414 (1999).
- <sup>30</sup>T. Ishihara, K. Tanaka, K. Fujita, K. Hirao, and N. Soga, *Solid State Commun.* **107**, 763 (1998).
- <sup>31</sup>G. N. Chapman and A. J. Walton, *J. Appl. Phys.* **54**, 5961 (1983).
- <sup>32</sup>H. Longchambon, *Bull. Soc. Fr. Mineral.* **48**, 130 (1925).
- <sup>33</sup>C. P. Keszthelyi and A. J. Bard, *J. Electrochem. Soc.* **120**, 1726 (1973).
- <sup>34</sup>V. E. Orel, Ya. Z. Opop, E. K. Goraiskii, I. V. Leshchinskii, and D. M. Khazanovish, *Medit. Tech.* **4**, 34 (1989).
- <sup>35</sup>K. Meyer, D. Obrikat, and M. Rossberg, *Krist. Tech.* **5**, 5 (1970).
- <sup>36</sup>K. Meyer, D. Obrikat, and M. Rossberg, *Krist. Tech.* **5**, 181 (1970).
- <sup>37</sup>T. Minami, *Ceramics* **32**, 36 (1997).
- <sup>38</sup>T. Minami, T. Maeno, Y. Kuroi, and S. Tanaka, *Jpn. J. Appl. Phys., Part 2* **34**, L684 (1995).
- <sup>39</sup>C. F. Yu and P. Lin, *J. Mater. Sci. Lett.* **17**, 555 (1998).
- <sup>40</sup>J. C. Ronfard-Haret, P. Valat, V. Wintgens, and J. Kossanyi, *J. Lumin.* **91**, 71 (2000).
- <sup>41</sup>S. Bachir, K. Azuma, J. Kossanyi, P. Valat, and J. C. Ronfard-Haret, *J. Lumin.* **75**, 35 (1997).